SENSOR

DEVELOPMENT OF HIGH RESOLUTION ULTRASONIC TRANSDUCERS FOR NONDESTRUCTIVE EVALUATION - PHASE 1

OCTOBER 31, 1987

B.M. HI-TECH INC.
P.O. BOX 97
COLLINGWOOD,ONTARIO,
CANADA L9Y 3Z4
(A SUBSIDIARY OF SENSOR TECHNOLOGY LTD.)

SENSOR
A subsidiary of
Sensor Technology Limited

B.M. Hi-Tech Inc.
P.O. Box 97, 12 Stewart Road,
Collingwood, Ontario
Canada L9Y 3Z4
Tel: (705) 444-1440

CONTRACT REPORT NO. 69102-01-SQ

DEVELOPMENT OF HIGH RESOLUTION ULTRASONIC TRANSDUCERS FOR NONDESTRUCTIVE EVALUATION - PHASE 1

Final Report

October 31, 1987

MICROMEDIA

WORK PERFORMED UNDER CONTRACT #15SQ.23440-6-9102 FOR
CANMET, MINERAL SCIENCES LABORATORY
DEPARTMENT OF ENERGY MINES AND RESOURCES
OTTAWA, ONTARIO

94pp

This report covers the research work titled "Development of High Resolution Ultrasonic Transducers for Nondestructive Evaluation - Phase 1" and is performed for CANMET, Mineral Sciences Laboratory of Energy Mines and Resources Canada.

The principal investigator for the project was Dr.S.E. Prasad. Other contributing authors are Dr.N.D. Patel and Miss. Tracy Klingbeil.

ACKNOWLEDGEMENTS

We would like to acknowledge the valuable discussions and the constant support received from Scientific Authority Dr.T.A. Wheat during the entire course of work. The authors would also like to thank Dr.A. Ahmad and Mr.A.G. McDonald for valuable help and suggestions.

ABSTRACT

ABSTRACT

The development of low dielectric constant, high piezoelectric coupling coefficient materials based on Lead Metaniobate is described. The design considerations required for the incorporation of these materials in high-resolution transducers for the non destructive evaluation (NDE) of advanced structural materials and the concepts for phased array systems are also described.

RÉSUMÉ

Le rapport porte sur le développement de matériaux à basse constance diélectrique et à haut coefficient de couplage, fabriqués à partir de métaniobate de plomb. Les auteurs donnent également un aperçu des calculs qui seront requis pour incorporer ces matériaux dans des transducteurs à haute résolution. Il s'agit de faire une évaluation par des essais non destructifs (END), des matériaux de construction avancés et des concepts de systèmes dotés de dispositifs à phases successives.

TABLE OF CONTENTS

TABLE OF CONTENTS

ACKNOWLEDEMENTS	i
ABSTRACT	ii
RESUME	iii
1. Nondestructive Evaluation of Advanced Ceramics	
1.1. Introduction	1
1.2. Ultrasonic Nondestructive Evaluation	3
1.3. High Frequency Techniques	5
1.4. Non-contact Methods	9
1.5. Conclusions	10
2. High Frequency Ultrasonic Transducers	
2.1. Introduction	11
2.2. Transducer Material Characteristics	11
2.3. Selection of Materials	16
2.4. Conclusions	19
3. Development of Piezoelectric Materials	
3.1. Introduction	20
3.2. Material Compositions	20
3.3. Ceramic Processing	21
3.4. Material Characterization	24
3.5. Conclusions	25
4. Design and Development of Prototype Transducers	
4.1. Introduction	27
4.2. Design Parameters	30

4.3. Technical Barriers 33

4.4. Fabrication of Prototype Transducers 34

4.5. Conclusions 35

5. Phased Array Transducers for the Nondestructive evaluation of Advanced Ceramics

5.1. Introduction 36

5.2. Principles 37

5.3. Acoustic Beam Pattern Control Techniques 38

5.4. Array Transducers 39

5.5. Technical Barriers for the Development of Array Transducers 40

5.6. Conclusions 41

6. Suggestions for Further Work

6.1. Material Processing 42

6.2. Ceramic Fabrication Techniques 42

6.3. Development of Transducers 43

7. References 44

APPENDICES

A1. Specification Data for Prototype Transducers

A2. List of Interim Reports Issued Under the Contract

CHAPTER 1

NONDESTRUCTIVE EVALUATION OF ADVANCED CERAMICS

1.1. INTRODUCTION:

The use of advanced ceramics in structural components such as gas turbines and diesel engines is increasing steadily. The US market for these components is anticipated to grow substantially over the next two decades from the present level of $50 million to over $5 billion US. The new developments will employ both sintered ceramics and composite materials.

In part, successful exploitation of advanced structural ceramic materials and composites in any application will depend on the use of a variety of quality control procedures to ensure that the product meets its specifications for minimum density, strength and physical homogeneity prior to assembly in any device such as an advanced gas turbine or an adiabatic diesel engine. It has long been known that the presence of sub-surface flaws in sintered ceramic degrades the mechanical strength and can initiate a crack propagation mechanism when the material is mechanically, electrically or chemically stressed.

The durability of advanced ceramic materials is dependent on ensuring that only physically homogeneous material is used and hence the need for nondestructive tests have come to the fore. Critical flaw sizes in ceramic turbine parts are very small. Detection of these small (< 5 micrometers) internal flaws is exclusively in the realm of ultrasonics. As such defects may not necessarily be linked

to the surface, dye penetration techniques are unsuitable. X-ray diffraction techniques are also unsuitable due to small defect sizes.

Ultrasonic nondestructive evaluation is considered a useful tool for the testing of advanced ceramics because of its ability to locate flaws in three dimensions and to determine their nature. Ultrasonic tests fulfill two basic requirements. Firstly, find the flaws, and secondly, characterize them as voids, inclusions or cracks, and above all, their size and orientation. Necessary frequencies for these requirements are an order of magnitude higher than normally used for industrial metals. Sound beams have to be focussed in order to obtain enough acoustic power; focal diameters are of the order of 0.5mm and scanning of a part can only be accomplished on a fully automated basis.

The transducers for higher frequency waves are less powerful than the more commonly used lower frequency ones, whilst the small flaws reflect less sound than the larger metal defects. This requires that ultrasound be concentrated utilizing a focussing mechanism so that an acoustic beam of less than 0.5mm diameter at focus is obtained. Conventional focussing is accomplished by transmitting sound pulses through a lens into water which has a very low attenuation. Upon entering a part with a higher sound velocity, the focussing cone shortens approximately as the ratio of the

velocities. For advanced ceramic components in water, this ratio is 8:1, limiting the maximum penetration to approximately 3mm.

Transducers for testing critical flaws in advanced ceramics are not commercially available. Further, the techniques for detecting and characterizing these defects must also be developed. To facilitate testing larger parts, development of variable focus phased array transducers are needed. Such transducers would allow for rapid initial scanning of large areas followed by a scan of suspect areas with enhanced resolution, thus reducing the costs greatly. Artificial intelligence techniques must also be developed for the analysis of data.

1.2. ULTRASONIC NON DESTRUCTIVE EVALUATION (NDE):

During the past ten years, nondestructive ultrasonic evaluation (NDE) of materials has become a powerful tool for the characterization of materials. Because of its simplicity of operation and greater depth of penetration, this method has several advantages over the other available NDE techniques. Ultrasound waves are sensitive to mechanical and elastic properties. Hence, grain boundaries and various crystallographic grain orientations are sources of contrast for ultrasonic transducers, even in unetched, polished polycrystalline samples that may be optically isotropic or anistropic. With optical and electron microscopy, it is difficult or impossible to check the distribution of different phases . Occasionally samples had to be thinned

down significantly to yield information, but again may not yield reasonable contrast. With acoustic microscopes, information can be obtained quickly and with reasonable contrast. Optical methods include detailed sample preparation and should have different refractive indices to obtain information. For example, in co-polymer or fibre-reinforced plastics, optical constants are similar but acoustic constants often differ significantly and thus result in high contrast acoustic images.

Mechanical properties of ceramic surfaces such as hardness, fracture toughness, and wear resistance are largely influenced by the behaviour of small flaws and defects. These may be due to microcracks, delaminations, voids as well as inclusions located beneath the surface. Acoustic microscopy or ultrasonic scanning is particularly suited to study these defects because it can see microscopic subsurface features without sectioning. Also from the measurement of velocity and attenuation of the leaky surface waves, one can closely correlate the mechanical properties of the material (1).

X-ray techniques can only detect a density difference of 1 % of the total sample used and therefore restrict the sample sizes. These techniques are also time consuming. Eddy current methods are limited to only conducting materials and so far it has been successfully deployed for the detection of surface discontinuities only. With surface cracks die penentrant methods can also be applied

successfully. However, these techniques are limited to crack openings greater than 50 μm wide. Ultrasonic NDE has the advantage that one can characterise both surface cracks and internal flaws and defects.

1.3. HIGH FREQUENCY TECHNIQUES:

For ultrasonic NDE of alloys, metals, plastic composites and medical ultrasonics, the transducer frequency ranges from 2.25 to 25 MHz. Recent findings led to the development of ceramics for high performance parts such as engines, cutting tools etc. These fine ceramic parts are made from SiC, Si_3N_4, Al_2O_3-SiC whiskers, ZrO_2 etc. Critical flaw size for such ceramics are very small and are typically less than 10 μm. Also machining ceramic parts creates surface flaws and thus increases the failure rate of such parts. Most common method used in testing the ceramic parts is proof testing. This method is destructive and also increases flaws as well as flaw sizing during testing. Ultrasonic NDE is the only technique capable of characterising such minute flaws. However, for the detection of small flaws and microcracks, high frequency sound waves in the region 50-150 MHz are required. As frequency increases, attenuation in the coupling medium (usually frequency-square dependence) and the test medium increase considerably. In order to overcome such losses, it is essential to design and develop low loss piezoelectric sensors, which is the aim of this project.

Most commercially available transducers have a lower frequency range of 0.1 to 25 MHz and a high frequency range of 0.3 to 5 GHz. If they are highly focussed, then depth of penetration is limited to a few tens of microns and depends upon the type of material under investigation. This problem will be discussed in detail later in this report. With a planar transducer, the signal scattered from the defects or flaws is very small and may be below the noise level of the electronic system. Therefore, one has to consider the problem carefully and develop the transducers accordingly. The transducer selection criteria will be discussed in detail in Chapter 2.

1.3.1. EARLIER WORK:

An acoustic microscopy study of ceramics coatings at 200 MHz was carried out by Yamanaka and co-workers (1). From the investigation on acoustic micrographs of the wear tracks of TiN film deposited on steel, it was concluded that after 1000 cycles of sliding contacts against a steel ball, a train of small circular cracks were discovered between the films and the substrates, when the film was deposited at relatively low substrate temperatures of 300 ^{o}C.

A scan system has been developed by Khuri Yakub (2) and his co-workers, to detect various defects in the range 25-500 µm range. Defect characterisation (size and shape) was carried out using information in both a time and frequency domain. Measurements were made in pitch catch mode and pulse echo scattering of elastic waves from Si and Fe inclusions in

Si_3N_4 in the frequency range 5-100 MHz . The inclusion sizes of 100-400 µm located 3 mm deep in materials were investigated. The scattering amplitude and the impulse response function were obtained by deconvolution of the reference waveform obtained by the reflecting and transmitting pulses from the back surface of the sample in a defect free region. A discussion was presented on the theory and experimental results. Defect characterisation (spherical voids and inclusions) has been carried out using A- and C-scan by Stockman (3) and co-workers. Shape information was gathered from A-scan whereas sizing characteristics were obtained from frequency domain using focussed 25 MHz transducers. It appears that to characterise defects/flaws of 10 µm or less, a frequency in the range of 50-150 MHz is required.

1.3.2. EXPERIMENTAL METHODS:

A- and C-scan ultrasonics is the way acoustic microscopes are used in principle. The technique uses the transducer as a transmitter and receiver. Conventional acoustic microscopes use highly focussed transducers, therefore restricting the depth of the penetration as shown in Figure 1.1. The depth of penetration depends upon the sound velocity of the test samples. According to Snell's law we have:

$$[\ (\sin\alpha 1/\sin\alpha 2) = C1/C2\ ] \qquad (1.1)$$

where C1 and C2 are sound velocities in different media and $\alpha 1$ and $\alpha 2$ are angles of incidence on the beam. If sound is

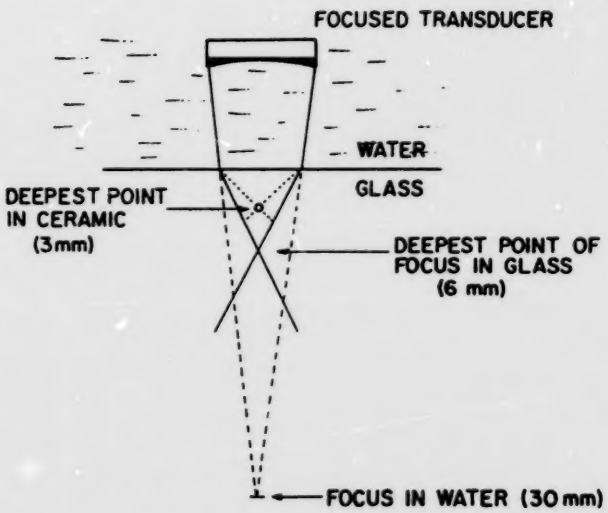

FIGURE 1.1. Focussing of Ultrasound

going from a low velocity medium (usually water, 1500 m/s) to high sound velocity medium at an angle, the refracted longitudinal wave will converge more towards the top surface in the test medium with increasing value of sound velocity in the test medium. The scanning acoustic microscope provides a unique combination of four features that make up its value for a wide range of applications, when compared to other techniques of microscopy.

(i) The method is non-destructive as it employs high frequency pulse, and therefore no visible damage is found on the test sample.

(ii) Ultrasonic sound waves can penetrate optically opaque material and the depth of penetration depends upon frequency, lens curvature and elastic properties of the material.

(iii) The information about density, adhesion, stiffness, viscosity and topography of the sample can be obtained from acoustic micrographs.

(iv) With optical and electron microscopy, the sample needs to be prepared which is time consuming. For example, the sample has to be optically polished and etched for grain study, whereas for this method, sample preparation is not necessary.

The scanning laser acoustic microscope (SLAM) utilizes another approach when compared with surface acoustic microscopes (SAM). Here a focussed laser beam is employed as an ultrasonic wave detector by virtue of the fact that

displacement at an insonified surface modulates light reflected from the surface and displacement is localized to the acoustic wavelength dimension. To produce an image the sample is insonified with a plane wave of ultrasound, and the laser is scanned rapidly over the field of view. The scanning rate is 30 images per second, which is 300 times faster that the rate achieved with the SAM'S mechanical device. However in both techniques a suitable coupling fluid must be employed to transmit sound waves and usually distilled water is used. The resolution capability of SLAM is generally limited to 0.5-1.0 wavelength in the sample. For example, at 100 MHz and using an aluminium sample the resolution is about 30 μm. However, at the same frequency, the SAM can produce a 10 μm spot in water at the surface of the sample. If the 10 μm spot is positioned at or up to a wavelength below the sample surface, then high resolution is obtained (see Figure 1.1). However at this high resolution it is not possible to go deep into the sample.

1.4. NON-CONTACT TECHNIQUES:

The necessity of providing mechanical coupling between a piezoelectric transducer and an object in which ultrasonic waves are to be generated presents a limitation in many ultrasonic applications. This is particularly true in N.D.E, where speed of scanning and ability to operate automatically as well as reproducibility under adverse conditions, including elevated temperatures, are highly desirable features of a transducer system. E. Papadakis (11) compared

a number of noncontact transducers which have recently been evaluated for NDE applications, including electrostatic transducers, electromagnetic transducers, and optical techniques based on the high power density or coherence of laser sources. Of these EMATS have been the subject of the most extensive development. These methods are useful for projectiles, steam generated tubes, and welds during fabrication. These methods are not fully developed to detect very minute flaws as discussed earlier.

1.5. CONCLUSIONS:

It can be concluded from the above, that there is a need for ultrasonic systems capable of penetrating deep into any sample with high resolution. This requires the development of an ultrasonic transducer with a high coupling coefficient and high intensity at high frequencies and high depth of penetration into the sample. To produce such transducers it is necessary to first develop highly efficient piezoelectric ceramics, and then design and optimize the transducer.

CHAPTER 2

HIGH FREQUENCY ULTRASONIC TRANSDUCERS

2. INTRODUCTION:

Recently many new piezoelectric materials combining a high electromechanical coupling factor with advantageous technological properties have been developed. The art of bonding thin plates of such material or their deposition by thin-film techniques onto suitable substrates has progressed to a state where devices operating at a centre frequency above 100 MHz with a large fractional bandwidth and low insertion loss can be readily fabricated. Such techniques have been reviewed by Meitzler (12). Before discussing the theoretical approach and practical aspects of transducer construction, a review of the available materials, their suitability and new direction in developing better materials is presented below.

2.2. TRANSDUCER MATERIAL CHARACTERISTICS:

Table 2.1 shows some selected materials and their properties for high frequency applications. These materials are selected in four categories.

(i) For thin-film applications ; materials such as CdS, ZnO, and AlN.

(ii) Piezoelectric single crystals such as $LiIO_3$, $LiNbO_3$ and $Ba_2NaNb_5O_{15}$.

(iii) Piezoelectric ceramics such as PZT, SPN, LMN and LT.

(iv) Piezoelectric polymers such as PVDF.

First category materials can be deposited onto suitable substrates with thin-film deposition methods such as vacuum

CHOICE OF MATERIALS FOR HIGH FREQUENCY TRANSDUCERS

	k_{33} %	Dielectric Constant	Acoustic Impedance $Tg/m^2.s$
SINGLE CRYSTALS			
Quartz	10	4.5	15
Lithium sulfate	38	10.3	11
Lithium niobate	45	30	34
POLYMERS			
Polyvinyl di fluoride (PVDF)	10	10	4
PIEZO-ELECTRIC CERAMICS			
Lead-ziroconate-titanate (PZT)	60-70	400-4000	30
Lead Metaniobate	40	300	20
Lead titanate	50-60	200	35
Sodium-potassium niobate (SPN)	42	400	31

TABLE 2.1. Material Parameters of Piezoelectric Ceramics.

evaporation, sputtering or chemical-vapor deposition techniques. In the second category, $LiIO_3$ is a water-soluble crystal combining a high coupling factor with a low relative dielectric constant. $LiNbO_3$ and $Ba_2NaNb_5O_{15}$ are ferroelectric and water insoluble crystals which combine a high coupling factor with moderate permittivity and very low dissipation loss. The third category represents ferroelectric ceramics with very high coupling coefficients, with high permittivity and high dielectric and mechanical loss.

Thin-film deposition techniques deposit a piezoelectric layer onto the substrate without the need for a seperate adhesive layer (which simplifies transducer assembly and avoids mismatch created by such layers). This method is capable of producing transducers well in the gigahertz range but constraints of material capability, chemistry and growth mechanisms have so far prevented the development of higher coupling factors (15). However, advancements in thin-film sputtering techniques have resulted in thick films of ZnO and AlN. High rate deposition of thick piezoelectric ZnO and AlN films have been achieved by Hata & co-workers (16) using magnetron sputtering techniques. With AlN, a plate thickness of several tens of microns has been obtained with a thickness coupling factor of about 17 % (17). A number of materials testing applications utilizing thin transducers have also been reported (18,19). In these, a 8 μm layer of ZnO is sputtered onto a 1000 $\mathring{A}$ thick gold film on a sapphire buffer rod. A second gold film on the ZnO layer completes the

electroding of the tranducer. The transducer center frequency was about 260 MHz with a functional band width of 80 %.

In contrast, thin-plate techniques are restricted to below 500 MHz , but yield transducers with coupling factors as high as the bulk materials. Since it is required to produce transducers in the frequency range of 50 to 150 MHz, our efforts will be concentrated in reviewing and developing materials for thin-plate techniques. Before going into details of this technique, let us examine the essential properties required of such materials for high frequency application.

2.2.1. DENSITY:

Apart from single crystals, if ceramics are used, then they should have densities greater than 94% of the theoretical value and a controlled grain size of 2-4 μm. The required thickness for 50-150 MHz for piezoelectric ceramics is 15-60μm. If the ceramics contain any pores on the surface, then current will concentrate at that area and cause break down of the sample during excitation. If the grains are larger, the material softens and grains pull out during lapping. During poling such grains introduce microcracking due to anistropy expansion. If the grain size is too small, then the piezoelectric properties decrease because of the surface charge effect. It is well documented in the literature that high coupling factors are attainable with maximum grain size in the range of 1 to 5 μm. Again

because of the grain size limitation of such ceramics, it can only be used up to 200 MHz due to the interference of vibrational frequencies of individual grains within the thickness mode.

2.2.2. RELATIVE DIELECTRIC CONSTANT:

As the thickness of piezoelectric element decreases, the capacitance of the element increases, thus creating a problem in electrical impedance matching. For example, if piezoelectric materials have relative dielectric constants of 200 and a thickness of 30 μm for a 100 MHz ultrasound probe, then only about a one-mm-diameter element can be effectively excited using impulse excitation. However, one can excite a larger diameter of about 4 mm, using a tone burst excitation where the exciting frequency is tuned to the transducer operating frequency. But in doing so, this method effectively decreases the bandwidth i.e. pulse length is increased, resulting in reduction of time resolution. Therefore, flaws near surfaces, or flaws together cannot be resolved properly. If high frequency, high power and short pulse (broad band pulse) is required, one has to have a very low relative dielectric constant.

2.2.3. ELECTROMECHANICAL COUPLING FACTOR:

For most NDE ultrasonic testing, compression wave transducers are used and the piezoelectric elements are used in the thickness mode. Therefore, high thickness coupling factor is desirable. Another mode associated with the thickness mode coupling via Poisson's ratio is the radial

mode and coupling coefficient k_p. This radial mode interferes with the thickness mode and thus distorts the pulse shape. Also much of the useful energy is spent in exciting such a mode. Therefore, one has to have almost zero radial mode coupling factor, i.e. a very high ratio of K_t/K_p. Ferroelectric crystals cited in Table 2.1 also possess this high unwanted radial mode factor.

2.2.4. ACOUSTIC VELOCITY:

In the application of high frequency compressional wave transducers, one should have a high thickness mode constant. This particular property helps in two ways:

(1) If velocity is higher, thicker elements compared with low velocity piezoelectric elements can be used at the same frequency. For example, piezoelectric materials having sound velocity of 6000 m/s and 4000 m/s, will have thickness of 30 and 20 μm respectively at 100 MHz. Thicker material will have good strength and can be handled easily. Also one can apply higher voltage to excite, thus increasing the final power output.

(ii) With thicker piezoelectric elements one has a low capacitance value compared with thin piezoelectric ceramics of the same permitivity. Thus, a larger diameter is permissible with a thicker element and the result is an increase in final power output. Although, having these two desirable properties, one has to sacrifice on acoustic impedance value,

which increases with the sound velocity. This creates an undesirable but solvable acoustic impedance matching problem with the acoustic damping medium.

2.2.5. MECHANICAL QUALITY FACTOR :

If very broad band transducers are desired without a damping back load, then piezoelectric material should have very low Q_m. PVDF, with a very low Q_m is a very useful material for exciting short pulses. Low Q_m is desirable, but not essential, since one can always design a proper backing medium to damp the ringing of the transducer to obtain a short pulse.

2.3. SELECTION OF MATERIALS:

From Table 2.1, it appears that ferroelectric crystals and PVDF have desired low permittivity when compared with piezoelectric ceramics. $LiIO_3$ is difficult to handle, since it is water soluble, whereas single crystals of $Ba_2NaNb_5O_{15}$ have shown high thickness coupling when compared with $LiNbO_3$. Earlier, the potential usefulness of $Ba_2NaNb_5O_{15}$ as a high frequency thickness transducer material was reported by Warner et al (20). Other advantages are a lower thickness mode acoustical impedance than those of $LiNbO_3$ and $LiTaO_3$ and the fact that the high coupling factor cut is a simple z-cut rather that a rotated y-cut. Upto 100^{o} C, the coupling factor is very stable. However, because of the cost, and small size of the crystals, no reports on transducer construction are cited in the available literature. The rotated y-cuts for

$LiNbO_3$ have particle displacement vectors within approximately 2 degrees of the ideal orientations. In practice, the unwanted mode lies more than 40 dB below the desired mode of transmission when these plates are used as bonded transducers (21). Nevertheless, most transducer manufacturers employ $LiNbO_3$ for high frequency transducers since no compatible piezoelectric ceramics are available commercially. 200 MHz line focus transducers were constructed by Khshibki et al (22) using lithium niobate crystals and acoustic sapphire lens with a cylindrical concave surface.

The use of the polymer PVDF as the element of a transducer generating and detecting ultrasound in solids has been demonstrated by Sussner et al (23) Ohigashi et al (24) and Alquie et al (25). Most transducers are for water coupling since acoustic impedance of their transducers is close to water impedance. Therefore, not much energy has been lost at the interface. Being flexible they can fit to complicated geometries and they are inexpensive. Focussed transducers (26,27) and arrays have been constructed with polymer films. When piezoelectric properties are compared with available piezoelectric material in Table 2.1 indicates that they are not efficient sound sources, but are sensitive sound receivers. Therefore, PVDF is a good hydrophone material. Characteristics of PVDF membrane hydrophones for use in the range 1-100 MHz was studied by Bacon (28) whereas analysis of the high-field losses of PVDF transducers in the

range 0.5 to 100 MHz were given by Chen (29). The low thickness coupling factor makes it an unattractive material for high-frequency transducers.

The piezoelectric ceramic transducers above 50 MHz create a fabrication problem because of the dimension of the elements. Preliminary investigations of highly dense piezoelectric ceramics have demonstrated that such ceramics in fact can be used for high frequency fabrication (30). A question arises here of whether we can decrease the dielectric constant of piezoelectric ceramics. There are two ways of solving such a problem:

(i) compositional modification

(ii) composite method of fabrication

A composition study of the system:

$$(Na_x Y_{1-x})_2 Nb_2 O_6$$

where Y is either Pb or Li and x varied in the range 0 to 1.0 should give information on permitivity. It has already demonstrated that LMN compositions provide some of the most favourable results for the high frequency work.

Gururaja & coworkers (31) have shown that by using materials such as BM532 and a polymer matrix, the permittivity of the composite can be brought down from 3200 to about 200. This will not effect the thickness mode coupling factor much but favourably reduces the radial mode coupling. Using a polymer matrix, both the density and acoustic velocity decrease. Therefore, acoustic impedance decreases and matches well with PVDF. However, composites

cannot be used for high frequency applications in their present form. If a ceramic or glass matrix is used, then perhaps one can bring the dielectric constant to a lower value, without greatly affecting the sound velocity. Also one can lap these materials more easily than polymer matrix materials.

Composites with polymer and glass matrices have been proposed for high frequency work but problems exist in both fabrication techniques and reliability of these materials. Existing data does not indicate a high frequency capability. The materials were however found to be extremely sensitive passive sensors.

2.4. CONCLUSIONS:

It can be concluded from the present review that ceramics offer potential opportunity for developing high frequency transducer materials. The lead metaniobate family of ceramics appear to be most favourable based on the material properties.

CHAPTER 3

DEVELOPMENT OF PIEZOELECTRIC MATERIALS

3.1. INTRODUCTION:

The term piezoelectricity refers to the phenomenon that electrical charge is generated when a force is applied to a ceramic material. The converse effect is also true and the ceramic undergoes mechanical deformation due to an applied electrical stress.

The ceramic materials are usually polycrystalline in nature and do not possess piezoelectric properties in their original state. They are composed of many crystals in random orientation with each unit cell containing dipoles. When a strong d.c. field is applied, the dipoles are aligned parallel to the field, making the ceramic piezoelectric. After poling, the ceramics exhibit specific electrical and physical properties like that of a single crystal of quartz or Rochelle salt. The piezoelectric materials investigated in the current programme have a specific crystal structure known as the perovskite structure.

3.2. MATERIAL COMPOSITIONS:

The piezoelectric ceramics prepared were specifically of two compositional formulations. These formulations have the general formula:

$$(A_x B_{1-x}) Nb_2 O_6$$

where A is Pb, Ba or Sr and B is Na, K, Li or Cd. The composition is generally known as lead metaniobate or PMN for short.

The compositions were systematically investigated over the range x=0.1 to 1.0; a total of 30 compositions were analysed.

Starting raw materials of carbonates and oxides of the above materials were used. The compositional formulas were used to determine the weights of each chemical required. Once the chemicals were accurately weighed out they were mixed thoroughly. All compositions were ball milled for 4 to 10 hours initially. The mixed slurry was then removed from the ball mill after several rinses with methanol and dried at 110 ^{o}C. Before calcining, each powder was screened through a 50 to 160 mesh screen to ensure uniform particle size.

All powders were calcined in large alumina crucibles at 600-1100 ^{o}C for 2-10 hours to remove any volatile material. As a precaution a weight loss determination was done for each composition analysed. After screening for a second time powders were ball milled in methanol, dried at 110 ^{o}C and finally screened again.

3.3. CERAMIC PROCESSING:

Each composition was mixed with a 5-20% solution of PVA (polyvinyl alcohol) binder using a mortar and pestle to assure uniform mixing before pressing. Discs of 1 inch diameter were pressed at pressures ranging from 10-25 MPa. The pressed discs were loaded into alumina crucibles and covered with the original powder to saturate the atmosphere inside the kiln. Saturation reduced the chance of lead loss in the PMN samples.

The firing cycle for the PMN compositions consisted of a ramp and soak cycle of the following: to 400 ^{o}C in 6 hours, to 1400 ^{o}C in 3 hours and the soak part of the cycle was experimented over the range 1000 ^{o}C to 1400 ^{o}C to evaluate the optimum sintering conditions for each of the 30 PMN compositions.

After firing, each sample was lightly polished using sand paper and then density measurements using Archimides principle (buoyancy technique) were taken. To determine density, the samples were weighed in air and then in water. The following formula was applied to obtain density:

Density = (Weight in air) / (Loss of weight in water).

Before applying brushed on silver electrodes to the fired samples, they were all thoroughly cleaned using toluene. The silver paint was applied to one side of each sample, then allowed to dry in an oven at 100 ^{o}C. The second side was then painted and left to dry. All edges were cleaned carefully with toluene. The samples were then fired in a mini kiln until a temperature of 400-700 ^{o}C was reached. After cooling, the samples were removed to be tested and poled.

The samples being analysed were all poled by applying 60-90 Volts per mil (one thousanth of an inch) of sample thickness. The poling tank consisted of an oil bath at an elevated temperature. Each of the samples were placed in the poling jig and the required voltage was then

slowly applied. The PMN compositions were poled for a time interval of 30 to 60 minutes. The maximum allowable current drawn by the samples was 1-2 mA.

Electrical measurements on all silvered samples were taken before and after polarization. The capacitance (C_b) and dissipation factor (D_b) were measured before poling. Then the dielectric constant of each sample was calculated using the formula $K=5.6617*T/(D^2)*C$ where T is sample thickness (inches), D is the diameter (inches) and C is the capacitance (pF). One day after poling, the capacitance and dissipation factor were measured once again as well as the piezoelectric charge generated by the sample. Using these voltage values, the piezoelectric strain constant known as d_{33} was calculated. The d_{33} value indicates that the piezoelectrically induced strain or the applied stress is in the 3 direction and the electrodes are perpendicular to the z axis. The formula used in calculating the d_{33} values was $d_{33}=V*(C1/C2)$ where C1 is the capacitance of the sample, V is the voltage and C2 is the capacitance of the standard sample. The dielectric constant was calculated after poling as well and was given the symbol . The results obtained for some typical compositions are listed in Table 3.1.

TABLE 3.1. PMN COMPOSITIONS

COMP	DENSITY (g/mL)	K (BEFORE POLING)	ε (AFTER POLING)	d_{33}
8702	4.70	740	512	90
8703	4.67	464	267	75
8705	4.57	*	*	*
8707	4.33	332	191	58
8708	4.24	248	162	42
8710	4.15	243	160	54
8712	4.31	232	208	12
8716	4.36	120	108	12
8721	4.08	43	46	9

* indicates a sample that could not be poled.

3.4. MATERIAL CHARACTERISTICS:

3.4.1. CRYSTAL STRUCTURE:

X-ray diffraction data indicated a well defined crystal structure with good peaks typical of the PMN structure. A typical x-ray spectrum is shown in Figure 3.1.

3.4.2. DENSITY MEASUREMENTS:

The PMN compositions yielded densities of up to 95 % of the theoretical calculated density. The lowest density recorded was 4.15 g/mL . It can be concluded from the results that the higher density samples do not necessarily give good electrical characteristics. For the compositions analysed, density increased directly with both sintering temperature and calcination temperature. At a sintering temperature of 1300-1400 ^{o}C along with a calcination temperature of 1000 ^{o}C, the compositions yielded their highest density values of 4.7 to 4.8 g/mL.

3.4.3. ELECTRICAL CHARACTERISTICS:

The PMN compositions were expected to produce samples having dielectric constants after poling in the range of 190 to 210 along with d_{33} values between 60 and 75. The original study of compositions at a firing temperature of 1200-1400 ^{o}C yielded promising results. From these data, three compositions were selected for further analysis. Batch sizes were increased to 600 g and each batch of powder was divided into three equal parts to be calcined at various temperatures to optimise the electrical characteristics of the samples. The best results overall were from composition 8707 which had

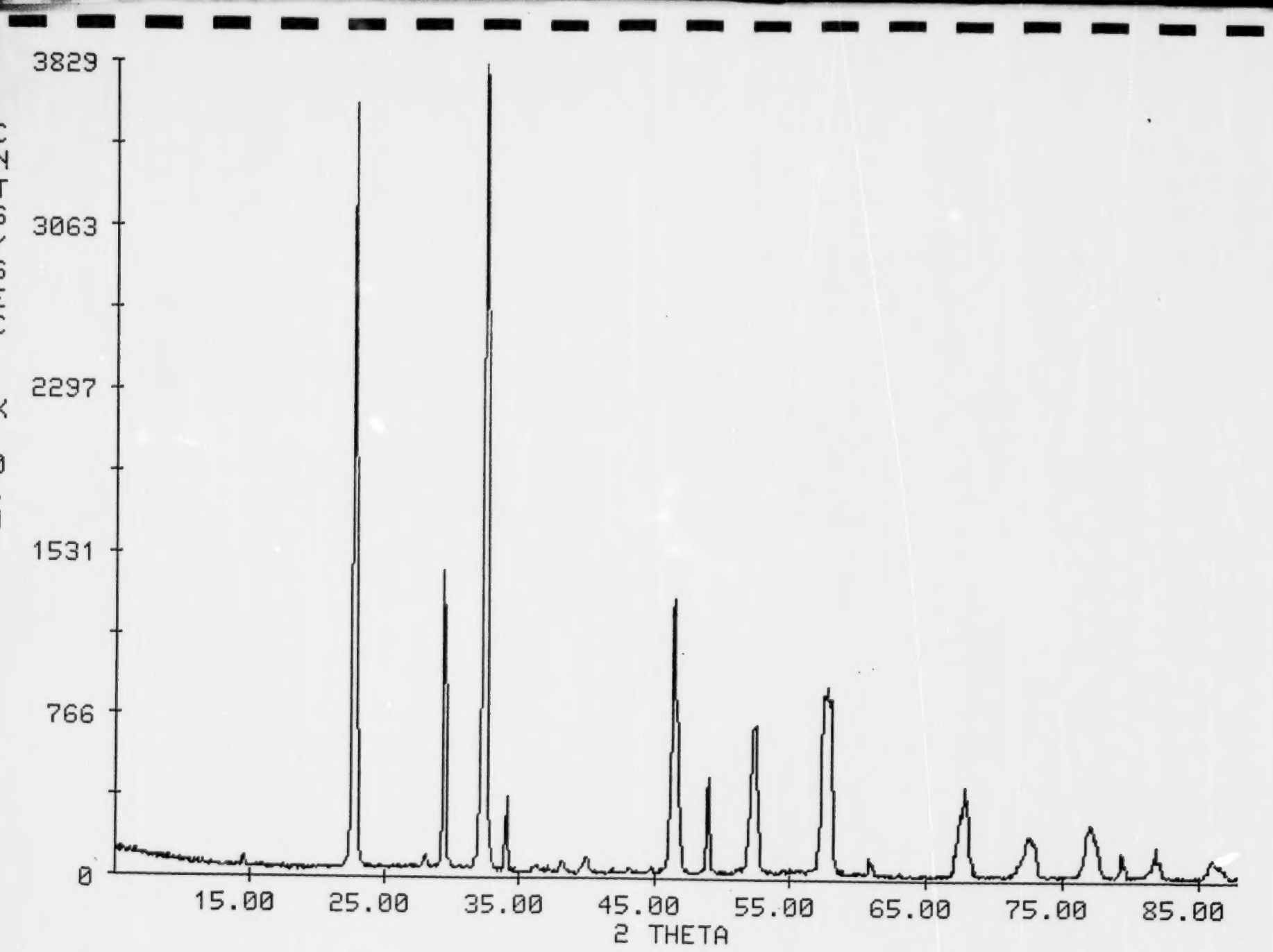

FIGURE 3.1 X-RAY DIFFRACTION PATTERN OF MATERIAL COMPOSITION 8707

a dielectric constant before poling (K) of 360, a dielectric constant after poling (ε) of 200 and a d_{33} value of 65. Since composition 8707 showed the most promising electrical results, two additional batches of powder were prepared under identical calcining and sintering conditions in order to investigate the consistency of the results. In Table 3.2, a summary of the electrical characteristics for each of the three batches is given.

3.4.4. AGEING CHARACTERISTICS:

The PMN samples had their electrical characteristics measured one day after poling. As an experiment, a selected number of samples were chosen and after several days their electrical measurements were taken once again to investigate their stability with time. In the case of PMN compositions, the dielectric constants remained constant over the time period however in most cases the d_{33} values decreased. In Table 3.3, the results from composition 8702 are listed.

3.5. CONCLUSIONS:

The most consistent results of the series of 30 PMN compositions were reported to be from composition 8707. Composition 8707 produced samples with exceptional electrical properties. The average density of these samples was 4.40 g/mL and the electrical characteristics were a dielectric constant of 200 and a d_{33} value of 65. During the current investigations, the reproducibility of these materials was established and the time stability evaluated. Some promising

TABLE 3.2. REPRODUCIBILITY CHARACTERISTICS FOR PMN8707

	BATCH 1	BATCH 2	BATCH 3
DENSITY (g/mL)	4.40	4.50	4.40
K	360	340	400
ε	200	205	210
d_{33}	65	60	60
C_B	350	260	320
D_B	0.020	0.025	0.030
C_A	190	155	180
D_A	0.010	0.010	0.015

K = Dielectric constant before poling; ε = Dielectric constant after poling; C_B = Capacitance before poling; D_B = Dissipation factor before poling; C_A = Capacitance after poling; D_A = Dissipation factor after poling.

TABLE 3.3. AGEING CHARACTERISTICS OF PMN8702 COMPOSITION

	ε	d_{33}
DAY 1	550	65
DAY 71	510	60
DAY 89	510	55

compositions have also been made with dielectric constants as low as 50. These materials have relatively lower d_{33} constants but the properties appear to be better than single crystal lithium niobate which is widely used today. Further investigations are in progress.

CHAPTER 4

DESIGN AND DEVELOPMENT OF PROTOTYPE TRANSDUCERS

4.1. INTRODUCTION:

The basic requirements of an ultrasonic transducer are its high sensitivity, resolution and a controlled radiation pattern. Several theoretical models for the design of such transducers have been proposed. These models may be grouped on the basis of their design emphasis and the assumptions made. Some designs treat the transducer as an unconstrained infinite anisotropic piezoelectric plate. The general field equations governing the vibration characteristics of such a plate are treated as due to electrical excitation (31,32). Such design methods are only applicable to transducers used as resonators. Other methods of transducer design use the equivalent circuit as a starting point (33). This type of design assumes that the wave particle displacements are parallel to the applied electric field and can be represented by a three-port electrical network. This is schematically shown in Figure 4.1. Both models described above yield similar results if appropriate assumptions are made and the relevant material constants are used (32).

A simple but effective approach to the design of an ultrasonic transducer is to consider the effect of component parts and the acoustic load on the ultrasonic parameters such as acoustic impedance etc (34). However such a method ignores both the piezoelectric properties of the element and the electrical characteristics of the device. The pulse response of the transducer can then be calculated from

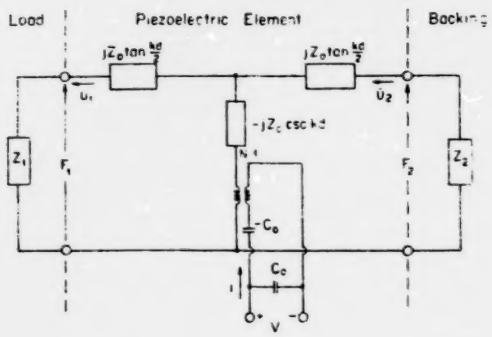

FIGURE 4.1. Equivalent Circuit for a Piezoelectric Thin Disc Transducer.

the successive delta function reflections of the various boundaries of the model. Considering a boundary between materials of respective acoustic impedances (Figure 4.2), Z_0 and Z_1, the reflected amplitude is given by:

$$(Z_0 - Z_1) / (Z_0 + Z_1) \qquad (4.1)$$

and the transmitted amplitude is given by:

$$2 Z_0 Z_1 / (Z_0 + Z_1) \qquad (4.2)$$

If the material Z_0 is a driven piezoelectric the amplitude in the piezoelectric is given by $Z_0/(Z_0 + Z_1)$ and that in the adjacent material by $Z_1/(Z_0 + Z_1)$. Combinations of these formulae are then used to drive the pulse height sequences in the receiver.

A variation of this technique was used at the NDT centre at Harwell, UK and involves a model in which pulse shape predictions have a cyclic rather than the simple delta function form. This is shown schematically in Figure 4.3 corresponds to a basic conventional ultrasonic probe consisting of a piezoelectric disc transmitting into water. The piezoelectric disc is assumed to be backed by a perfectly absorbing material. The major limitation of this type of model is that the electronic nature of the transducer is ignored with the result that the transfer of energy to and from the electrical circuitry is not taken into account. With low frequency transducers (below 25MHz) one can almost ignore the electrode thickness effect, but other bonding media (bond line, wear plate etc) may seriously effect the above model.

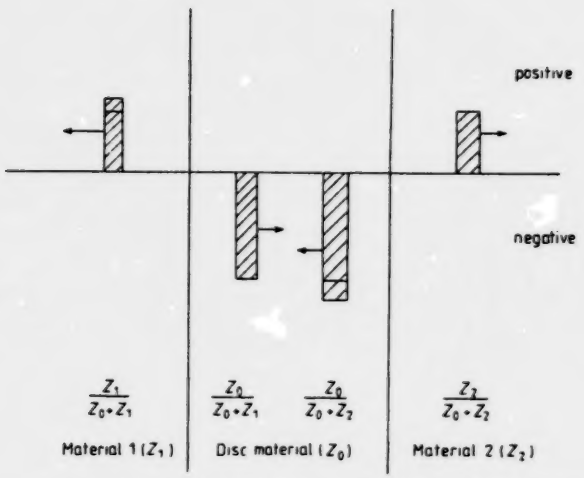

Distribution of ultrasonic amplitude from a piezoelectric disc. Stylised pulse distributions at an instant after the application of the driving pulse are shown above formulae governing the partition of amplitude at the surface of the disc.

FIGURE 4.2.

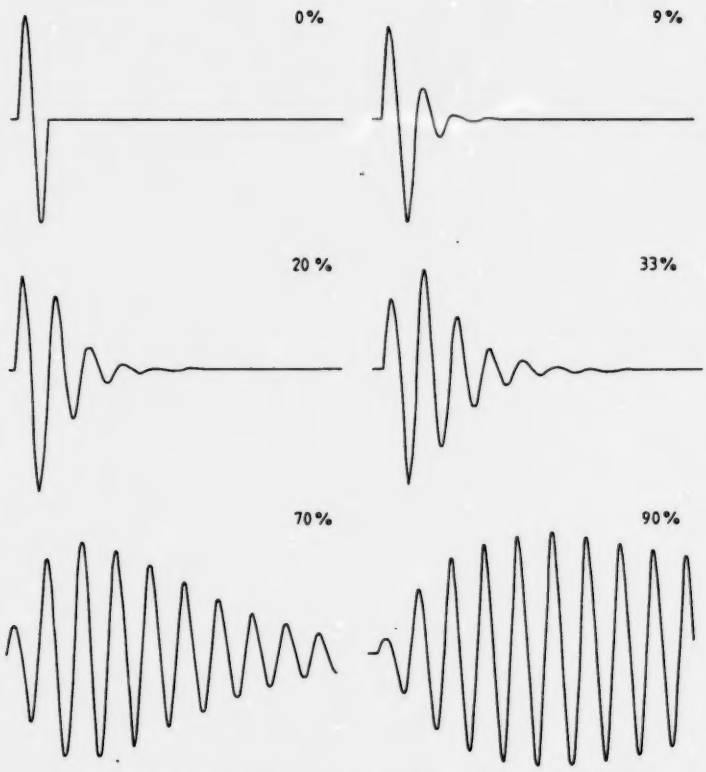

Simple calculations of pulse shape variations as a function of rear face reflectivity.

FIGURE 4.3

The basic ultrasonic probe for NDE by compressional waves consists essentially of a piezoelectric material bonded to some form of backing block (Figure 4.4A). The latter provides the necessary mechanical support and, in addition, serves to dampen the oscillations of the generally highly resonant transducer element. The construction of such probes to provide repeatably a desired response is, however, by no means simple. Such a transducer can be represented schematically by a layered structure as shown in Figure 4.4B.

The equivalent circuit approach also lends itself quite naturally to the analysis of a composite layered transducer structure consisting of the piezoelectric element, the electrodes, backing materials, wear plate, radiating layers and the medium into which the sound wave is transmitted. An equivalent circuit for this type of multilayered transducer was developed by Sittig (35,15). It consists of tandem connection of two-port networks each representing one of the layers. For each of these networks, a two-by-two complex transmission matrix, of input and output parameters of the layers, is formulated. The transmission characteristics of the entire device may then be expressed in terms of a chain matrix obtained by multiplying all of the transmission matrices of the individual layers. Such a method is also used to evaluate the transient response of a transducer (36). An alternative method was developed by krimholtz, Leedom and Matthaei (34). The outline of this model is schematically shown in Figure 4.5. The

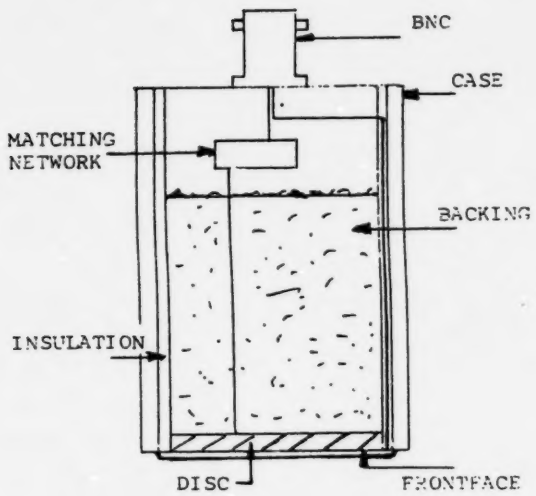

FIGURE 4.4A Baisc Structure of an Ultrasonic Transducer, based on a Piezoelectric Disc Resonator.

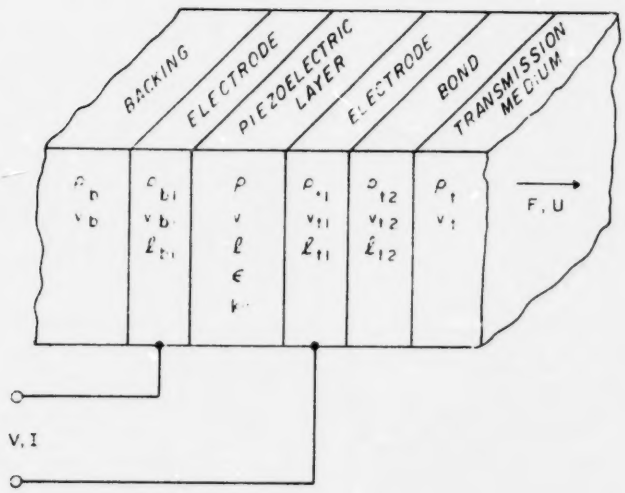

Multiple layer configuration necessary in practice to drive a transducer and to affix it to the transmission medium. Layer data: Normalized impedance $Z_n = \rho_n v_n / \rho c$. Normalized thickness $t_n = c_n l / c l_n$.

FIGURE 4.4B

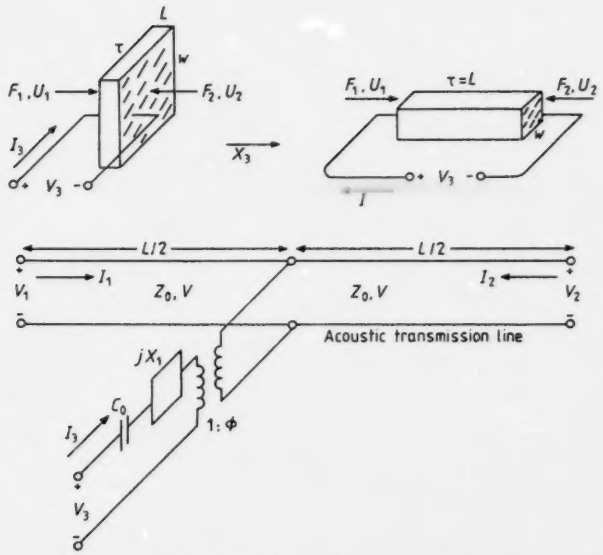

The equivalent circuit developed by Krimholtz, Leedom and Matthaei for both a thickness expander plate and a length expander bar with end electrodes. $C_0 = \tau w/(\beta_{33}{}^S t)$, $V = V_t{}^D = (C_{33}{}^D/\rho)^{1/2}$, $Z_0 = \tau w V_t{}^D$, $\phi = (1/2M)$ cosec $(t\omega/2V_t{}^D)$ and $X_1 = Z_0 M^2$ sin $(t\omega/V_t{}^D)$ where $M = h_{33}/(\omega Z_0)$.

FIGURE 4.5

piezoelectric element is represented here as a lossless acoustic transmission line and coupled at its mid point to a lumped network representing the electrical properties of the disc. Any other layer can be added to these acoustic outlets as required by the transducer design under investigation. The model has been evaluated by numerous investigators but information regarding the applicability of this model to very high frequency transducers is not available.

4.2. DESIGN PARAMETERS:

Some of the factors which are involved in the design of a transducer have been given in Table 4.1. The most important design problem is the preparation of the piezoelectric element and its attachment to a suitable absorption backing material so that the acoustic energy can pass from the piezoelectric disc into the backing with little or no interfacial reflection, and very high damping characteristics.

The damping of an impulse train is determined by the acoustic impedances of the backing and of the medium coupled onto the front face of the transducer. When the impedance of the backing is made equal to the impedance of the disc (perfect matching) the transmitted ultrasound consists of two equal and opposite impulses. The pulses are emitted from the front and back surfaces of the mounted disc and are therefore seperated by the time, t, required for propagation through the thickness of the disc. This may be expressed as:

$$\tau = t/C \qquad (4.3)$$

Transducer component	Characteristics
Disc material	Curie point Dielectric constant Geometry Acoustic impedance Polarization Homogeneity
Electrodes	Configuration Mechanical strength Electrical conductivity Chemical stability Molecular diffusion Thin layer behaviour Wire welding ability
Backing material and front surface modification.	Damping characteristics Mechanical adherence Acoustic impedance Particle shape and size distribution. Melting point Aging
Electrical connections	Contact wires connector (to lead or leads). Matching network
Housing	Geometric design and strength. Sealing against water etc.

TABLE 4.1. Piezoelectric Transducer Design Parameters

where t is the thickness and C is the compressional wave velocity in the piezoelectric material (Figure 4.6).

In general, after initial excitation, stress waves ψ and β undergo multiple partial transmission and reflections at the transducer/external media interface. Assuming the transducer is in perfect contact with medium A and B, calculation of the form of pulses transmitted to the latter is, however, straightforward using simple transmission and reflection coefficients coupled with time delays in multiples of τ. With the transducer and medium B together now taken to represent a probe working into a test material, represented by test medium A, it can readily be established that, firstly, a square pulse of duration τ is the shortest pulse that can be transmitted to medium A and, secondly, that this pulse can only be obtained if medium B (now assumed to be probe backing) is a perfect acoustic match to the transducer. Notice that, whilst amplitudes may vary, under the latter condition the shape of the pulse transmitted to the test material is always the same regardless of the acoustic impedance of the test material.

According to Bragg's law of diffraction which defines the maximum attainable resolution in terms of wavelength,

$$d_{min} = \lambda/2 \qquad (4.4)$$

the shortest pulse that can be achieved will be half the wavelength and is given by:

$$\tau = \lambda/2 \qquad (4.5)$$

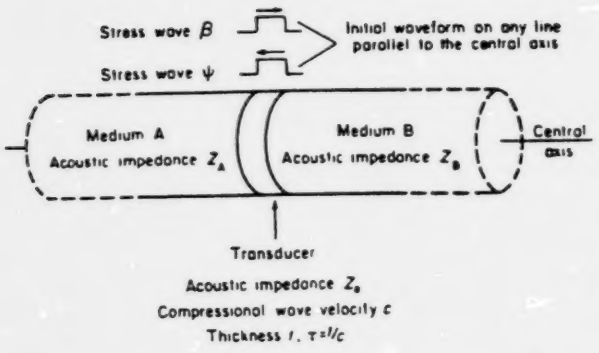

Amplitude transmission coefficients

$$T_{(\text{transducer} \longrightarrow \text{medium A})} = \frac{2Z_A}{Z_0+Z_A}$$

$$T_{(\text{transducer} \longrightarrow \text{medium B})} = \frac{2Z_B}{Z_0+Z_B}$$

Amplitude reflection coefficients

$$R_{(\text{transducer} \longrightarrow \text{medium A})} = \frac{Z_A-Z_0}{Z_0+Z_A}$$

$$R_{(\text{transducer} \longrightarrow \text{medium B})} = \frac{Z_B-Z_0}{Z_0+Z_B}$$

FIGURE 4.6. Transducer Response to Delta Pulse Current Input

where $\lambda = C/f$, f being the frequency of the transducer.

The following equations may be used for calculation of probe bandwidth:

$$Z_f + Z_b \simeq \sqrt{2}\, Z_p k_t \qquad (4.6)$$

where Z_f is the impedance of the backing layer

Z_b is the impedance of the backing medium

Z_p is the impedance of the piezoelectric material

and k_t is the thickness coupling.

With ceramic elements, usually a designer cannot satisfy the requirements of the equation 4.6 and the transfer at the front face cannot be maximized. Three methods can be used in the practical fabrication of the transducers. In the first type of design, the material constants are chosen such that the equation 4.6 is satisfied. For immersion transducers (in water) this may be achieved with polymers such as PVDF. The second type design employs a backing material such that $Z_b \simeq 0.7Z_p$. In this case the low value of Z_f is irrelevant to the bandwidth performance of the transducer. This is the most common method used in the commercial manufacture of transducers. Finally, transformation of the value of the combined input impedance of the mechanical circuit which loads the ideal transformer is achieved by the introduction of the near quarter wave matching layers, to bring the combined load close to the value specified by Equation 4.6.

4.3. TECHNICAL BARRIERS:

One can use the above models to predict the transducer parameters and design good transducers with predictable pulse shape and power. However, the physical dimensions of the piezoelectric elements (60μm at 50 MHz), thickness of the matching and backing layers at very high frequencies makes their fabrication very difficult. Bonding between the piezoelectric disc and the absorbing backing material should also be good. Such a problem can be solved by using indium bonding. With such bonding techniques, one has to start with thicker piezoelectric ceramics, then gold and indium electrodes are successively applied to the ceramic disc and the bonding medium. These are then pressed in vaccum under a pressure of 50-100 psi. The other face of the piezoelectric material is then lapped to the required thickness. However, with this technique, it is difficult to connect electrical wires for excitation. Also the backing material (usually metal loaded polymer) will deform slightly, thus reducing the possibility of good bonding. Such a design has been found very useful in the assembly of saphire or quartz delay line bonded transducers where no backing materials are required. Another approach is to bond a very fine wire to the active electrode diameter of the piezoelectric disc and then mold the backing medium onto this plate. Precautions must, however be taken to eliminate any air bubbles.

The selection of electrode diameter is very important in the case of ceramic elements having various dielectric constants (30). The signal strength as a function of optimum electrode diameter are shown for BM830 (sodium potassium niobate) (Figure 4.7A) and BM8707 (Leadmetaniobate) ceramics (Figure 4.7B) are shown. These ceramics have dielectric constants 425 and 200 respectively. Optimum electrode size may be obtained by performing a series of experiments to measure the signal strength as a function of electrode diameter. Once the optimum dimensions are exceeeded the signal strength decreases and the pulse shape is distorted.

The piezoelectric properties of ceramic elements change with their surface to volume ratio. Figure 4.8 shows the variation of d_{33} constant for BM8707 ceramics as a function of thickness. Repoling does not restore the values to the original levels. These are some of the effects that must be taken into consideration in the design of the fabrication of high frequency transducers.

4.4. FABRICATION OF PROTOTYPE TRANSDUCERS:

BM8707 elements were selected to fabricate the prototype transducers. A centre frequency of 50 MHz was used in the design of the transducer. Ceramic discs 7mm diameter and about 0.8mm thick were selected from lot of poled units. They were bonded to a flat quartz plate and using the quartz plate as a support, the elements were lapped to 62 µm thick corresponding to 50MHz. Gold electrodes of 2mm dia were sputter deposited and the elements were checked for the

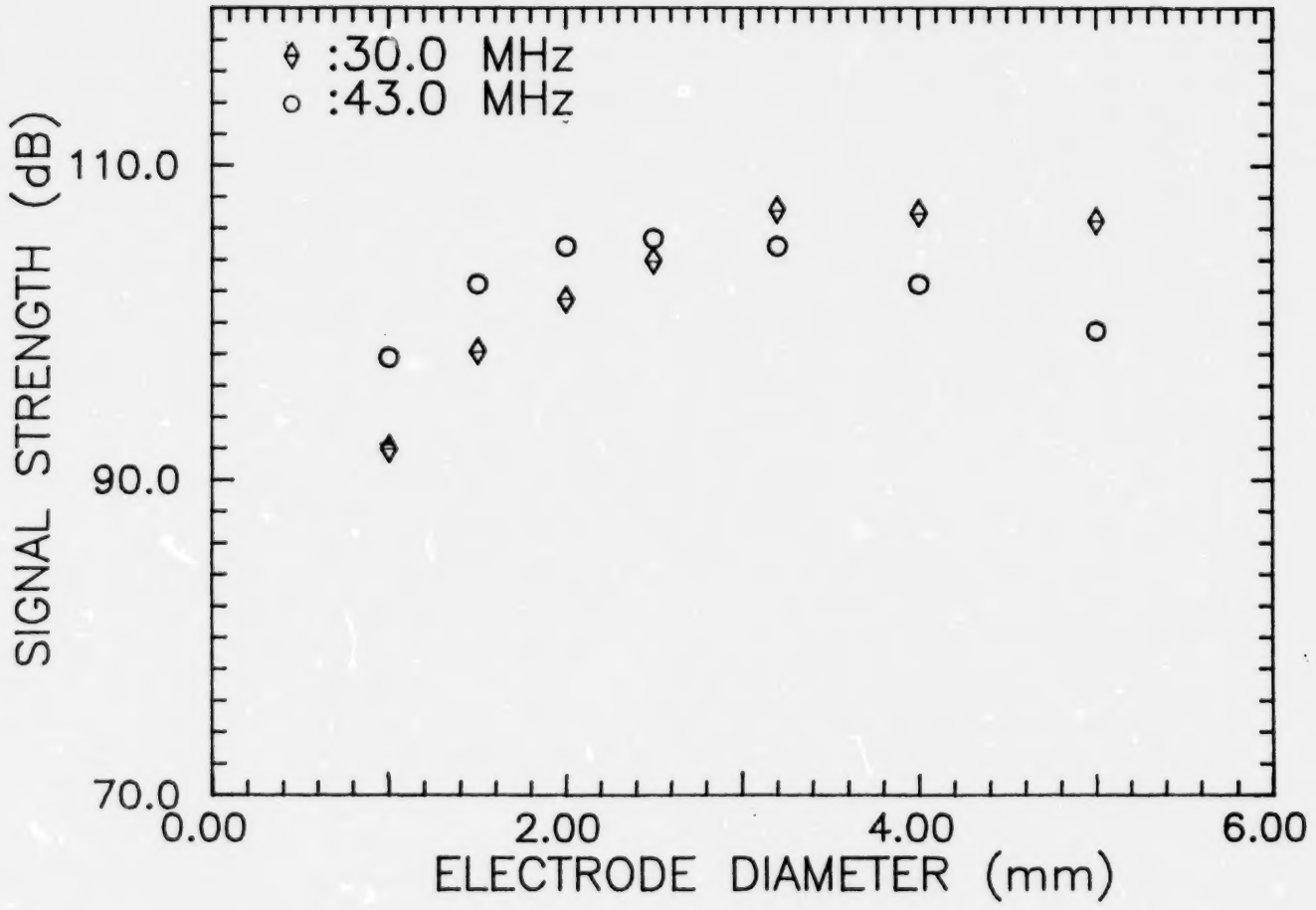

Figure 4.7A. Signal strength as a function of electrode diameter at different frequencies for BM8707 elements

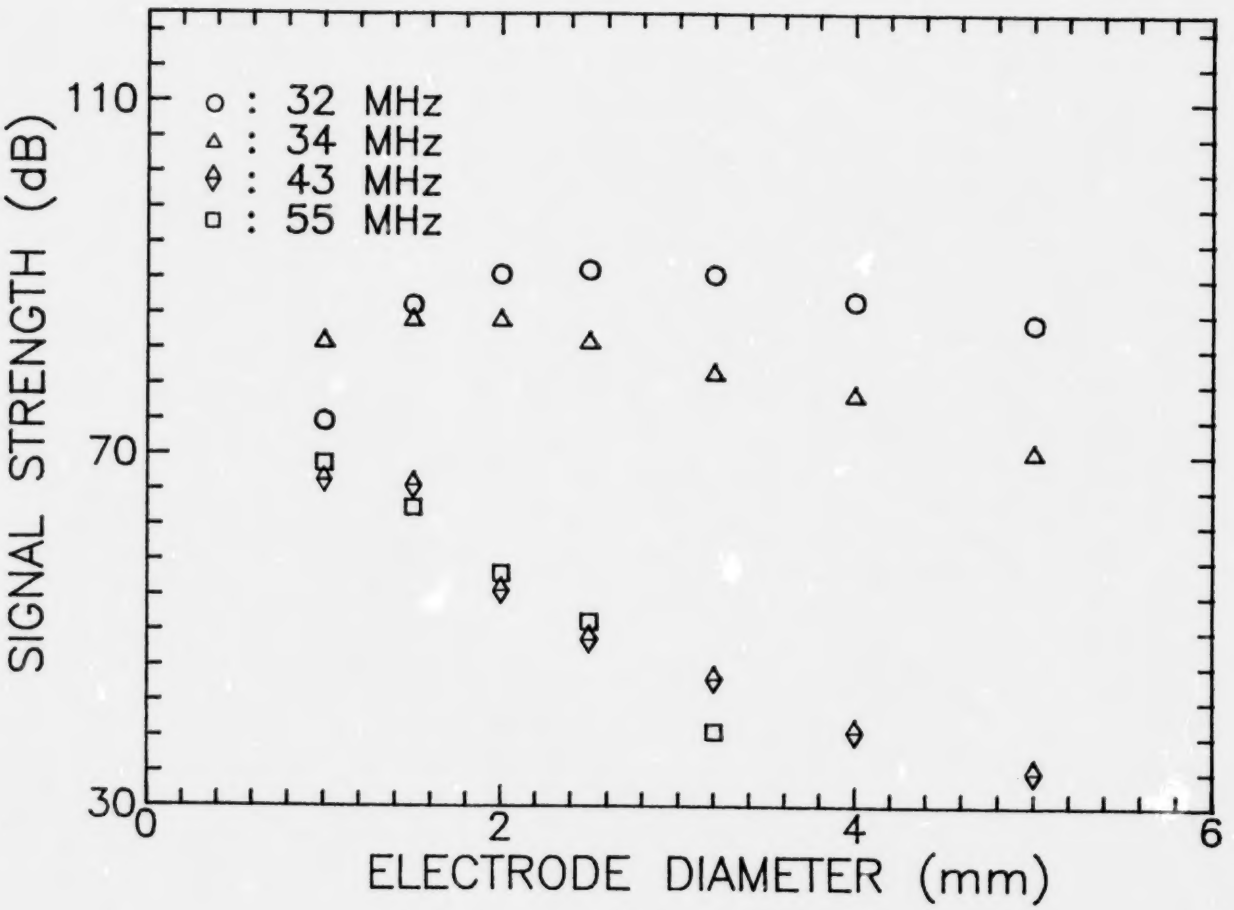

Figure 4.7B. Signal strength as a function of electrode diameter at different frequencies for BM830 Ceramics

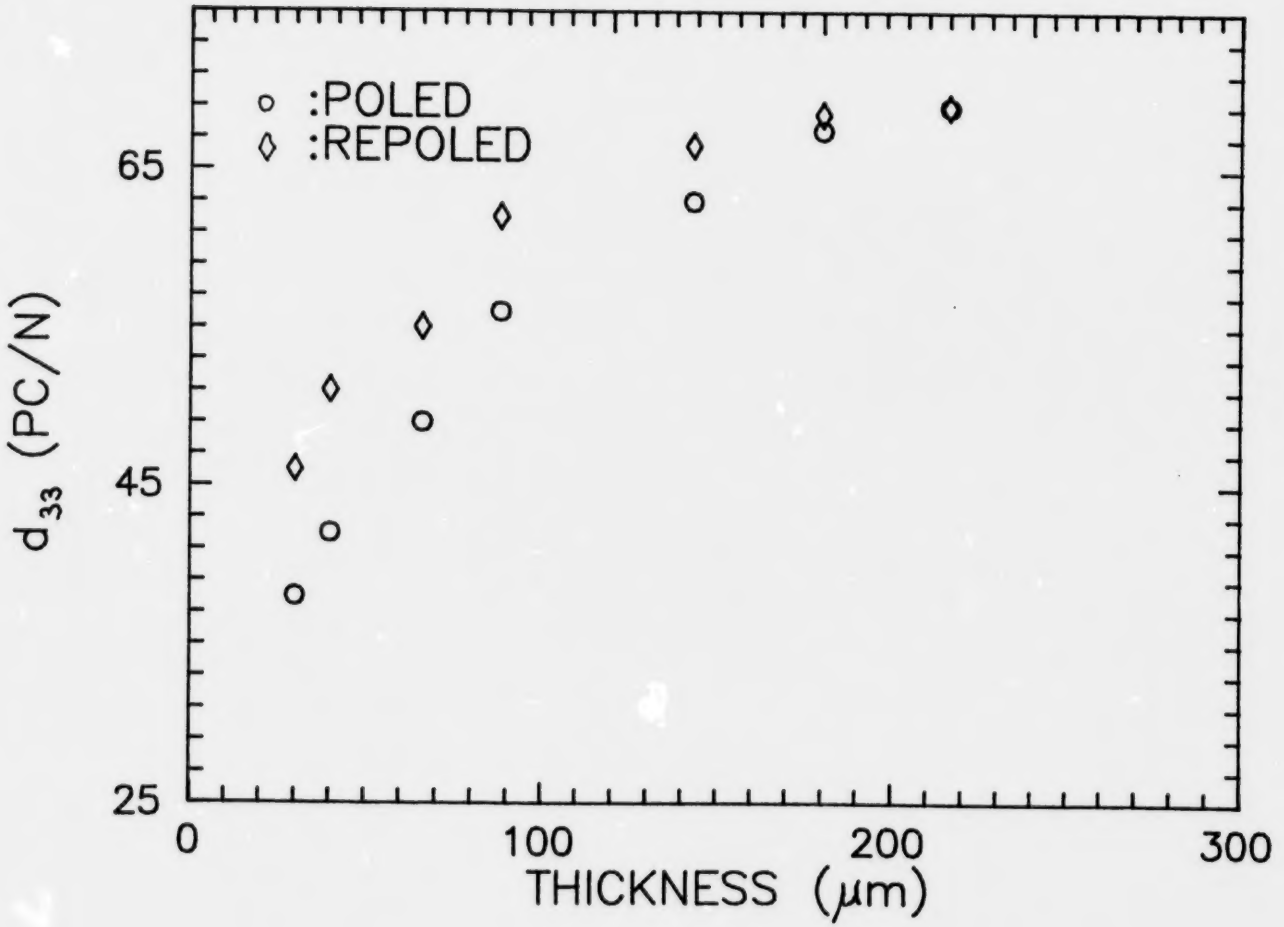

FIGURE 4.8. Variation of piezoelectric coefiicient d_{33} for BM8707 as a function of thickness. The effect of repoling on these ceramics is also shown

electrical characteristics and signal strength before their assembly into transducers.

A copper wire 150µm in diameter is now attached to the ceramic element with silver epoxy. Stainless steel rings of 9mm OD and 8mm ID were placed concentrically with the elements as shown in Figure 4.9. The backing material consisting of tungsten loaded epoxy was poured to fill the steel rings. The assembly was removed after curing and tested for its performance by mounting into a temporary housing and obtaining the beam profile by scanning with a 2 mm pin target in water. The final mounting in the housing is then completed. The front face of the transducer is covered with a layer of polymer and then gently polished to a quarter wavelength (2-3 µm) matching. These transducers were evaluated in both time and frequency domains as well as the beam profile were recorded and the data is included in the appendix A1.

4.5. CONCLUSIONS:

High frequency transducers models have been developed and the technical barriers for the production of the same have been identified. Prototype transducers have been assembled and characterized for their performance.

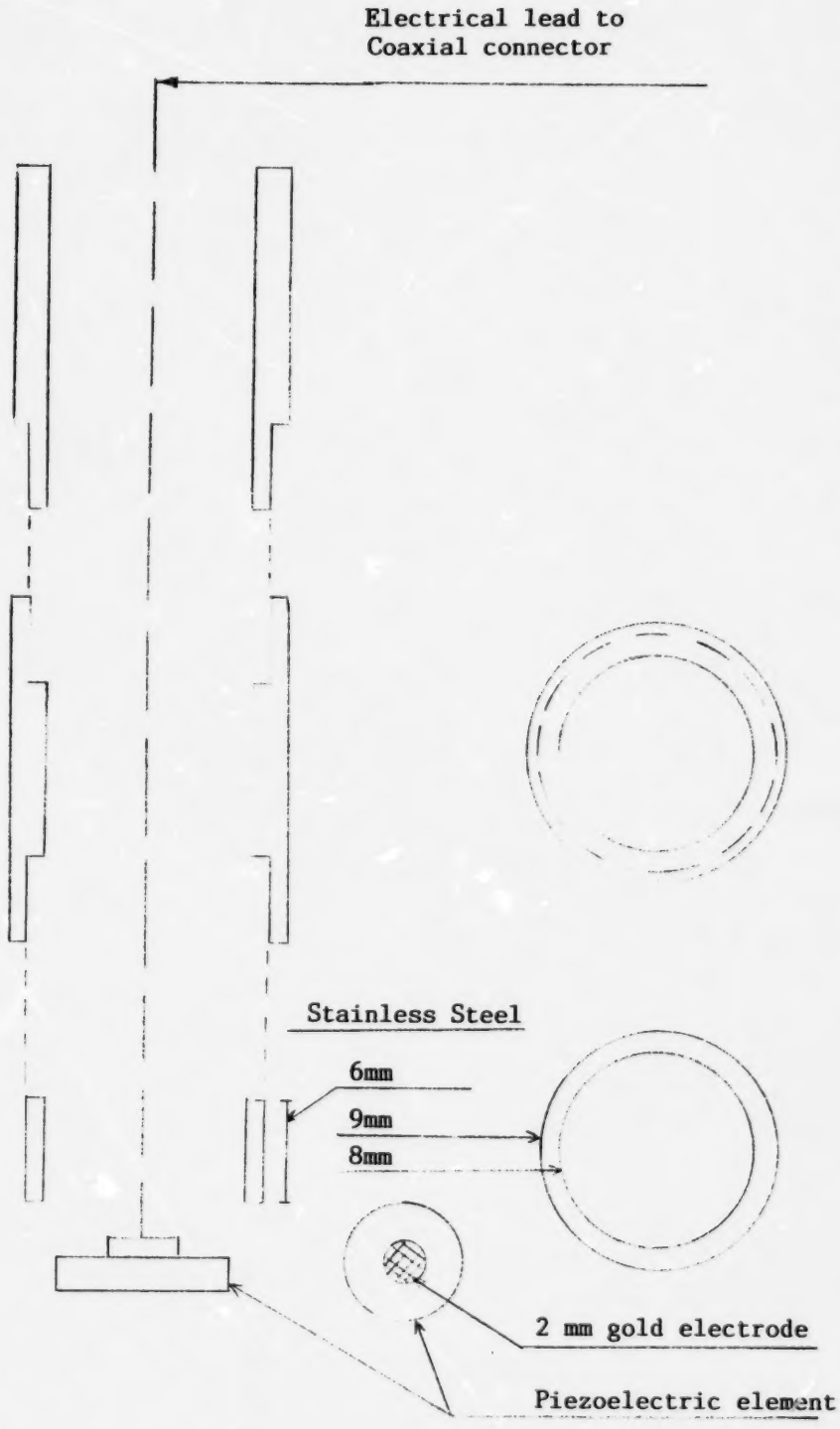

FIGURE 4.10. Design configuration of the prototype high frequency transducer.

CHAPTER 5

PHASED ARRAY TRANSDUCERS FOR THE NONDESTRUCTIVE EVALUATION OF ADVANCED CERAMICS

5.1. INTRODUCTION:

The use of phased arrays offers an alternative means of focussing ultrasonic transducers and of varying the angle of the acoustic beam. The advantages of an array over a single element transducer can be summarized as follows:

The arrays are more sensitive since a number of transducer elements operate in the same sound field.

The arrays possess directional properties that enable them to discriminate between signals from different directions.

The array has an improved signal-to-noise ratio over a single element transducer since it discriminates against isotropic or quasi-isotropic noise in favour of a signal arriving in the direction that the array is pointing.

These advantages suggest the use of transducer arrays in potential applications involving nondestructive evaluation of advanced ceramics.

Simple sources and uniformly vibrating spherical shells radiate energy equally in all directions and therefore have no directional characteristics, but distributed arrays of sources or receivers, or extensive surfaces serving as such, have unique radiation patterns. Pattern control serves a number of useful properties and is a major design problem. Most obvious is that the concentration of beam not only

provides a higher intensity level but also gives directional information. This is particularly useful in target location and beam steering. By the use of phasing techniques beams may be shifted, split, rotated or otherwise manipulated to obtain information or guidance advantages.

5.2. PRINCIPLES:

Multiple probe arrays typically consist of a number of small transducer elements of width comparable to or smaller than the ultrasonic wavelength as shown in Figure 5.1 (34). Each element of the array is excited by a similar driving pulse but a time delay for excitation elements can be provided electronically. Such excitation will generate a combined wave form as shown in Figure 5.1. The Huygens construction may be used for these waves. The net result is that of an ultrasonic beam at an angle θ and is given by:

$$\theta = \mathrm{Sin}^{-1}\left[\frac{c\,\Delta t}{w}\right] \qquad (5.1)$$

where c is the ultrasonic velocity in the medium and w is the centre to centre width of the element in the array. This formula implies no limit to the value of the angle of the ultrasonic beam and in principle a tangential beam ($\theta = 90$) is possible at a value of Δt given by :

$$\Delta t = [\ \pi w/2c\ ] \qquad (5.2)$$

For still greater values of Δt there is no general region in which all of the transmitted waves are in phase.

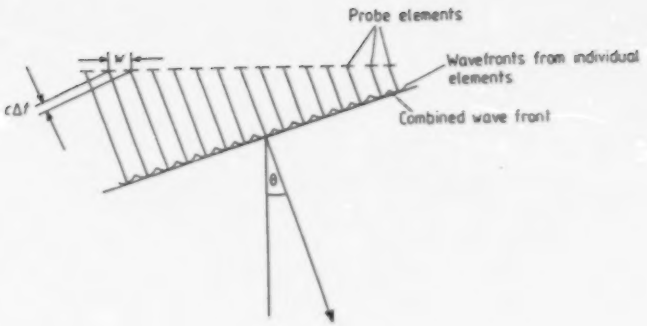

FIGURE 5.1. Principle of operation of a Phased Array Transducer

5.3. ACOUSTIC BEAM PATTERN CONTROL TECHNIQUES:

The response of a transducer array varies with direction relative to the array. This property of array directionality, as discussed in the previous sections is highly desirable. This is due to the fact that it enables the direction of arrival of a signal to be determined as well as resolves close and adjacent signals. Directionality in transducer arrays results from the fact that sinusoidal signals arriving in a direction tend to be in-phase at all the array elements. Similarly, broadband signals arriving in this direction tend to be correlated between pairs of any elements. This direction of maximum in-phase condition or correlation is that of an acoustic axis of the arrray and is the direction of maximum sensitivity (37).

Arrays can normally be steered either mechanically or physically by rotating the array, or electrically by a phase delay for narrowband devices and time-delay for broadband devices. This results in effectively rotating the direction of maximum response into some desired direction.

Beam steering is achieved in a transducer by the introduction of delay lines as shown in Figure 5.2(a). The sound beam is steered by rotating the acoustic axis of the line through the angle ϕ. Numbering the elements zero to N, a delay equivalent to a phase lag of $Nkd \sin\phi$ is introduced to element N, where k is the wavenumber, d is the distance

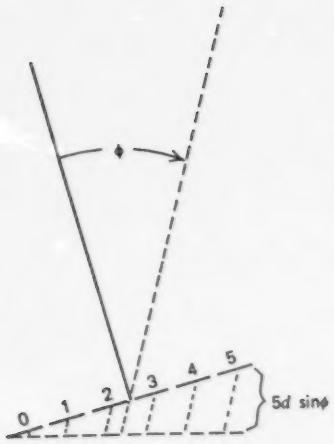

A. A phase shifted array

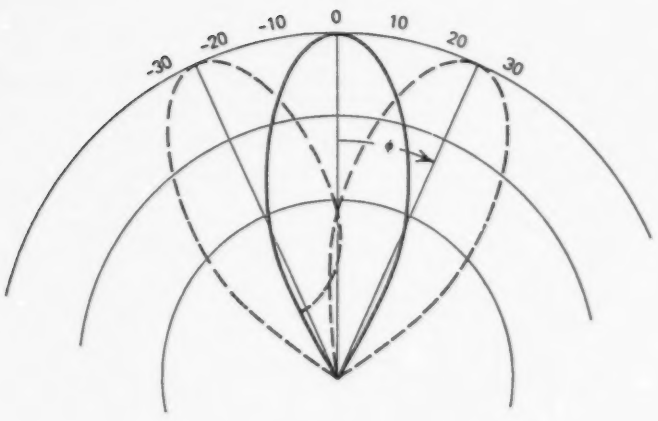

B: Shifted lobe pattern

FIGURE 5.2

between elements and Φ is the angle from the normal to that the beam is steered. This is schematically shown in Figure 5.2(b).

Figure 5.3 illustrates an effect gained by manipulating the amplitudes by which the segments of a line are driven. Such beam patterns are obtained by making amplitudes for all elements equal (solid pattern) or varying in proportion to the coefficient of each term (dashed lines). Such a control is also known as 'shading'.

An alternative means of exciting the elements in the linear array would be to delay the inner element excitations with respect to the outer elements. Figure 5.4(a) shows the results when a simple constant time relationship Δt is employed and it can be seen that a degree of beam focussing can be achieved. The focussing can be made even more perfect if the time delay between the individual elements is varied. This is schematically shown in Figure 5.4(b).

5.4. ARRAY TRANSDUCERS:

The usefulness of array transducers has been discussed in the earlier section. An introduction to potential applications of such transducers is presented here. The single element line arrays are useful in many applications but the addition of an orthogonal plane adds considerably to the versatility of the source. As indicated in Figure 5.5 a variety of sources may be assembled on a plane. The figure also shows points that may represent simple sources, line segments, or circular or rectangular

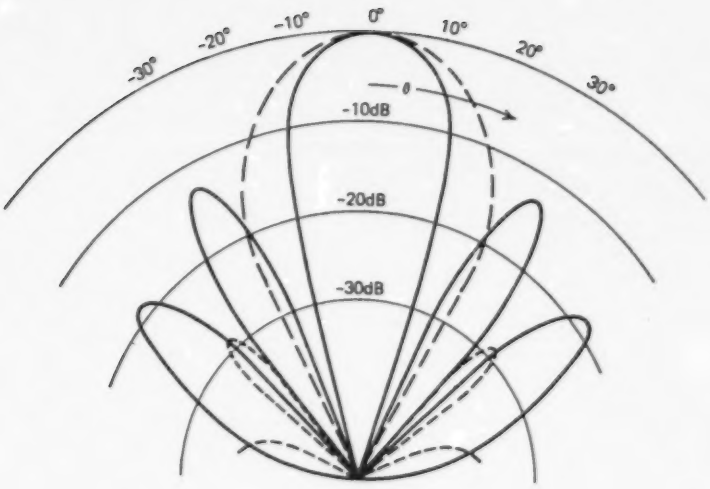

FIGURE 5.3. Control of beam pattern by the variation of amplitudes of excitation of elements.

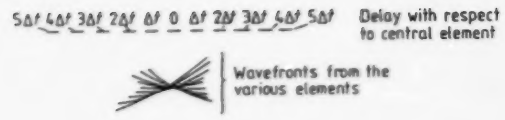

5.4A. Fixed time delay between elements

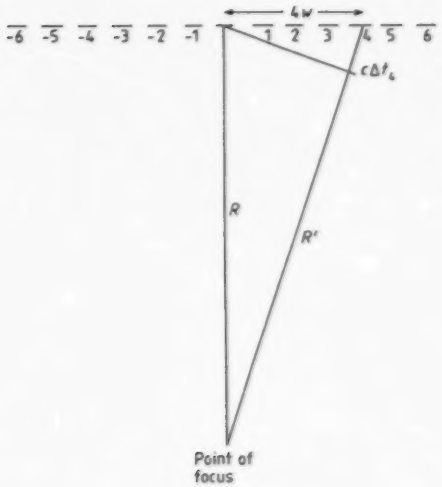

5.4B. Variable time delay between elements

FIGURE 5.4. Principle of time delay excitation method of focussing multiple transducer arrays.

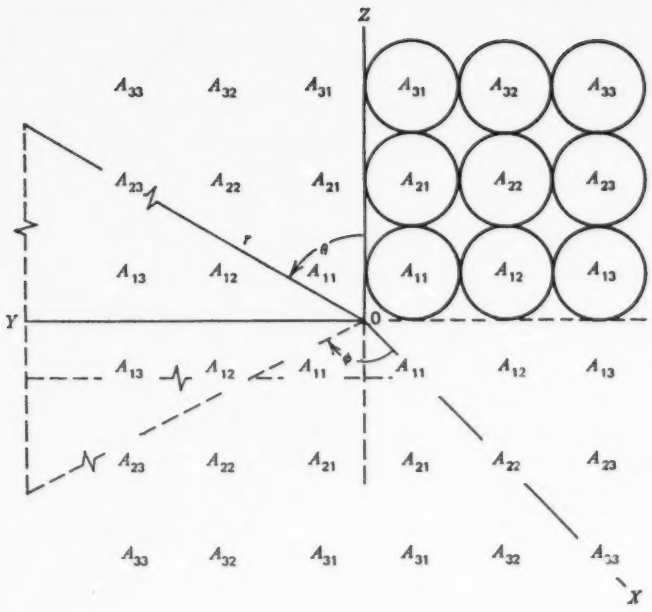

FIGURE 5.5. A plane array

surfaces. Figure 5.6 shows a section from a cylindrical array of transducers. By inserting time delays equivalent to that required for a signal to travel in the test medium the distance between each element and the chord AB, the cylindrical section approximates a plane array and is responsive to similar methods of pattern control.

In the foregoing sections array transducers that are both linear and additive types have been discussed. These transducers are made up of elements that have an output linearly proportional to the acoustic pressure and which are simply added together to give an output. Instead of adding element outputs, they may be multiplied together and averaged so as to form a correlative array (38). Such concepts are schematically shown in Figure 5.7. This technique is appealing in applications where a reduction in the number of elements is necessary. Here the physical size and the number of elements may be traded off for complexity in processing.

5.5. TECHNICAL BARRIERS IN THE DEVELOPMENT OF PHASED ARRAY TRANSDUCERS:

With array transducers, the beamwidth, array gain and resolution are all interconnected. The Huygens type of construction does not take into account the variation of the intensity in the ultrasonic wave as a function of angle. Thus although equation 5.1 may correctly predict a beam angle, it could well be that insufficient energy is emitted at this angle to allow the beam to be useful in

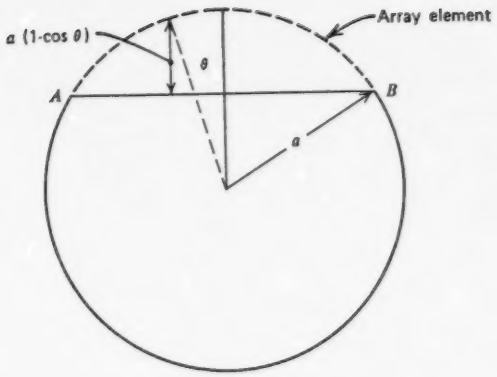

FIGURE 5.6. A cylindrical array.

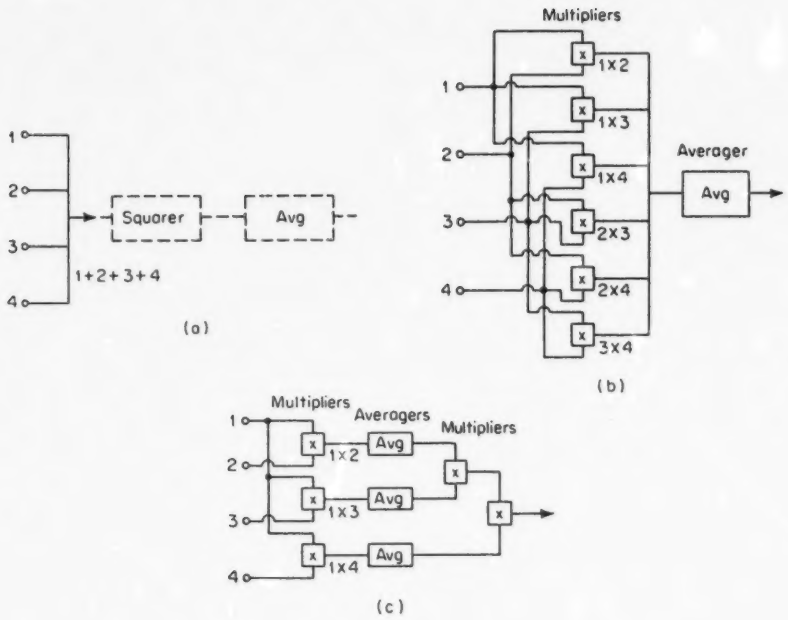

FIGURE 5.7. Correlative array concepts. [a] additive array, [b] intraclass correlator and [c] total average product (TAP) array.

nondestructive evaluation. Further, such a model assumes that the pulse emitted by the transducer elements is short. In reality, most ultrasonic pulses are cyclic so that the initial positive cycles will be followed by other positive cycles at a separation in spatial terms of one wavelength. This means that other conditions of constructive interference may occur. Multiplicative or correlative arrays will overcome some of these problems but at the expense of processing complexity. Correlative methods are also useful only at high signal-to-noise ratios, since the effect of noise is to destroy the beam pattern unless a long averaging time is used.

5.6. CONCLUSIONS:

Array transducers offer the advantages of good resolution, good signal-to-noise ratio and acoustic beam steering capability. Correlative processing can also be used with such transducers. However, to realize the capabilities offered by such transducers, it is necessary to eliminate conditions of constructive interefence. This may be achieved by the design and development of short pulse transducers which in turn require development of appropriate acoustic damping materials and damping techniques.

CHAPTER 6

SUGGESTIONS FOR FURTHER WORK

6. SUGGESTIONS FOR FURTHER WORK:

Based on the review of the status of technology for the nondestructive evaluation of advanced ceramics and the new piezoelectrics developed during the current programme, further work should be undertaken in the following areas.

6.1. MATERIAL PROCESSING:

A detailed examination of compositions in the system $(Na,Li)NbO_3$ where very low dielectric constants have been observed, will be useful. Such materials may eventually replace the much widely used single crystal materials due to their low cost and other advantages.

During the current investigations, two compositions have been identified as most suitable for utilization in transducers. A further study of these two compositions, $(Pb,Na)Nb_2O_6$ [BM8707] and $(Na,Li)NbO_3$ [BM8720] would be useful, particularly in the area of development of oxide and non-oxide precursors as well as scaling up of batch sizes.

Further improvement of properties of ceramics may be achieved through pressure sintering of the ceramic compositions developed. Investigations in this area will be useful.

6.2. CERAMIC FABRICATION TECHNIQUES:

At high frequencies, geometrical irregularities produce spurious effects in the transducer output. A systematic evaluation of precision lapping techniques, grinding and

geometry control, production of special geometries such as annular shapes for transducers such as catheters would be useful.

6.3. DEVELOPMENT OF TRANSDUCERS:

During the current phase of research, it has been established that fabrication of prototypes of transducers is feasible. A detailed design report outlining the materials, fabrication, evaluation and systems for operation of these transducer is useful.

The need for broadband transducers for single or half pulse operation has been identified in the report. Realization of such transducers will include development of acoustic matching materials, delay lines and development of encapsulation systems. Any further work in this area should include the development of these components.

Phased array transducers offer the potential of utilizing the high frequency transducer technology into practical systems. Detailed design analysis and development of models similar to those on high frequency transducers is useful. Fabrication of prototype transducers in the low megahertz range may provide a starting point in their development.

CHAPTER 7

REFERENCES

7. REFERENCES:

1. Yamanaka, IEEE Ultrasonics Symp.- Atlanta, GA. 1983

2. Yamanaka, IEEE Ultrasonics Symp.- New Orleans 1973

3. Khuri-Yakub, IEEE Ultrasonics Symp.- Atlanta, GA. 1983

4. Stockman, A.J. & P.S. Nicholson, Private Communication

5. Lee, S., Heeley J.D., Mahern J.M. & Orgavecs L.M.G., IEEE Trans. on Sonics & Ultrasonics Vol. 30 No. 2,1983.

6. Petts, C.R. & Wickramasinghe, H.K., Electronic Lett. Vol. 16 p. 9, 1980.

7. Hadimioglu, B. & Quate, C.F., Applied Physics Lett. Vol. 43 p. 1006 1983.

8. Guangoi, Y., Nikoonahad M. & Ash, E.A., Electronic Lett. Vol. 18 p. 767 1982.

9. Nikoonahad, M., Yue, G.Q. & Ash, E.A., Electronic Lett. Vol. 19 p. 782 1983.

10. Lemons, R.A. & Quate, C.F., 'Physical Acoustics' Vol. XIV., Acedemic Press pp. 2 - 90 1979.

11. Papadakis, E., IEEE Ultrasonic Symp.- Phoenix, AZ. 1977.

12. Meitzler, A.H., 'Ultrasonic Transducer Materials' - O.E. Mattiat, ed., Plenum, New York 1971.

13. Sensor/B.M. Hi-Tech. Product Bulletin.

14. Pennwalt Corporation, PA., USA.

15. Sittig, E.K., 'Physical Acoustics' - Mason & Thurston, ed.Acedemic Press pp. 221 - 272 1972.

16. Hata, T., Takeda, F., Morimoto, O., Noda, E. & Hada, J. Jpn. J. Appl. Phys. Vol. 20 Suppl 20-3 pp. 145-8,1981.

17. Shiosaki, T.,Yamamoto, T., Oda, T. & Kawabat, A., IEEE Ultrasonic Symp. - Boston,1980.

18. Khuri-Yakub, B.T. & Kino, G.S., Ultrasonic Symp. Proc. IEEE, Cat. No.:76 CH 1264-1 SU.,p.564, 1976.

19. Khuri-Yakub, B.T. & Kino, G.S., Ultrasonic Symp. Proc. IEEE., Cat. No.:77 CH 1264-1 SU., p.53, 1977.

20. Warner, A.W., Coquin, G.A., Meitzler, A.H. & Fink, J.L., Appl. Phys. Lett. Vol. 14 pp. 34-35,1969.

21. Warner, A.W. & Ballman, A.A., Proc. IEEE 50, p. 450 1967.

22. Khshibki, J., Ohkubo, A. & Chubachi, N., IEEE Ultrasonic Symp.- Chicago, IL. 1981.

23. Sussner, H., Michas, D., Assfalg, A. & Hunglinger, S. Phys. Lett. Vol. 45 p. 475, 1973.

24. Ohigashi, H., Shigenari, R., & Yokota, M., Jpn. J. Appl. Phys. Vol. 14 p. 1085, 1975.

25. Alquie, C., Lewiner, J., & Friedman, C., Appl. Phys. Lett. Vol. 29 p. 69, 1976.

26. Bennet, S.D. & Chambers, J., Electronic Lett. Vol. 13 p. 110, 1977.

27. Chubachi, N. & Sannomiya, T., Ultrasonic Symp. Proc. IEEE., Cat. No.:77 CH 1264-154. pp. 119, 1977.

28. Nakamura, K. Shimizu, H. & Sato, N., [illegible]s. on Sonics & Ultrasonics., Vol. Su-30 No. 6 p. 345 1983.

29. Chen, W.H., IEEE Trans. on Sonics & Ultrasonics., Vol. Su-30 No. 4 p. 238, 1983.

30. N.D. Patel & P.S. Nicholson, Private Communication.

31. Tiersten, H.F., J.Acoust. Soc. Am. Vol.35,53, 1963; Linear Piezoelectric Plate Vibrations, Plenum, NY, 1969; Ultrasonics, Vol.8, 19, 1970.

32. Meeker, T.R., ultrasonics, Vol.10, 26, 1972.

33. Mason, W.P., Electromechanical Transducers and Wave Filters, van Nostrand, 1948.

34. M.G. Silk., Ultrasonic Transducers for NDE, Adam Hilger, 1984.

35. Sittig, E.K., IEEE Trans. Son. Ultrason., Vol. Su14, 167, 1967; Vol. Su16, 2, 1969.

36. Papadakis, E.P., J.App. Phys., Vol. 42, 2990, 1971.

37. Principles of Underwater Sound for Engineers,
R.J. Urick, McGraw Hill, 1967.

38. Underwater Acoustics
L.W. Camp, Wiley-Interscience, 1970.

39. A. Fahr, Private Communication.

APPENDIX A1

SPECIFICATION DATA FOR PROTOTYPE HIGH FREQUENCY TRANSDUCERS

B.M. HI-Tech Inc.

High Frequency Ultrasonic Transducer
for Nondestructive Evaluation

Centre Frequency: 50 MHz

Element effective diameter: 2mm

Housing: Stainless Steel

Electrical Termination: Standard BNC

Tuning circuits: None

Operating Temperature: $-25^{o}C$ to $+40^{o}C$

[This is a prototype transducer. Precautions must be taken with respect to excitation voltage, intepretation of data etc. The ultrasound beam characteristics are shown in Figures A1.1 and A1.2.]

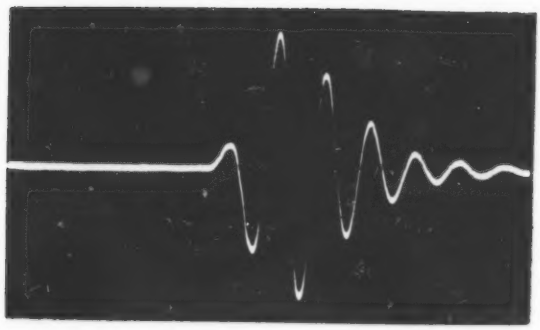

A. Real time waveform of the transducer

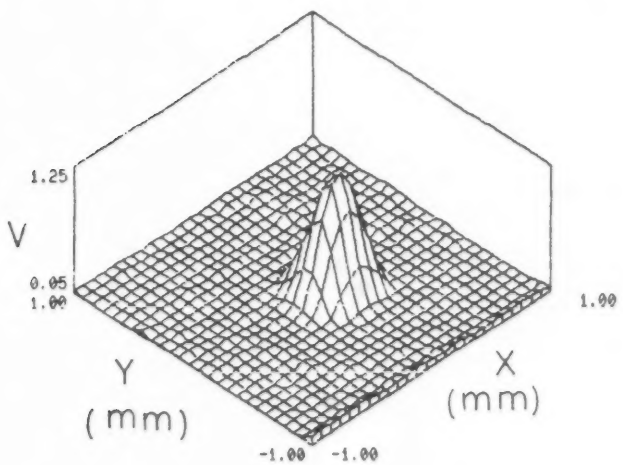

B. Local beam strength profile

A1.1. Characteristics of prototype 50MHz transducer

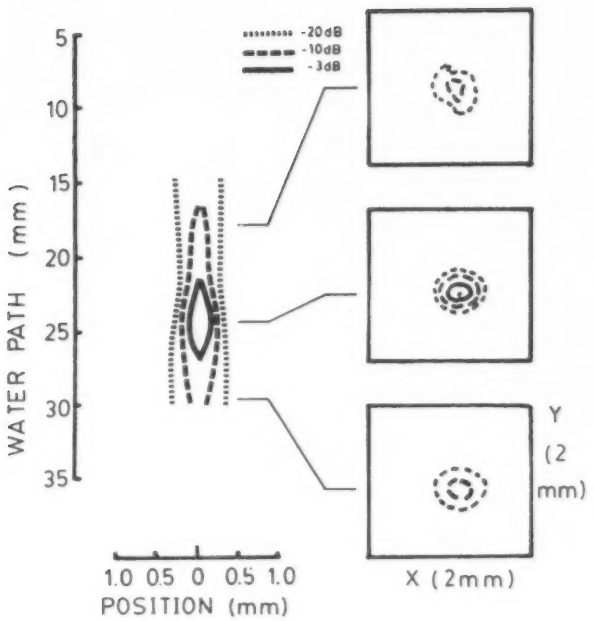

FIGURE A1.2. Field Strength in focal zone of the prototype transducer.

APPENDIX A2

LIST OF INTERIM REPORTS ISSUED UNDER THE RESEARCH PROGRAMME

LIST OF INTERIM REPORTS ISSUED UNDER THE RESEARCH PROGRAMME

1. Review and Assessment of Transducer Materials and Techniques; 31 March 1987.
2. Development of Piezoelectric Materials; 15 June 1987.